Gamma-Ray- and Neutron-Induced Photocurrent and Readout Noise in LYSO+SiPM Packages

Chen Hu, *Member, IEEE*, Nan Lu, Liyuan Zhang, *Member, IEEE*, Ren-Yuan Zhu, *Senior Member, IEEE*, Adi Bornheim, Lautaro Narvaez, Jason Trevor, and Maria Spiropulu

***Abstract*— $Lu_{2(1-x)}Y_{2x}SiO_5$ (LYSO) crystals readout by a silicon photomultiplier (SiPM) will be used in the barrel timing layer of a precision timing detector for the Compact Muon Solenoid (CMS) experiment at the High-Luminosity Large Hadron Collider (HL-LHC). This detector is expected to be exposed up to 5-Mrad γ-ray dose, 2.5×10^{13} charged hadrons/cm^2, and 3×10^{14} n_{eq}/cm^2 at the HL-LHC for 10 years of operation. We present results of the photocurrent in LYSO+SiPM packages induced by Co-60 γ-rays and Cf-252 neutrons of the expected dose rate and neutron flux, respectively. The γ-ray-induced readout noise is about 30 keV, which is negligible when compared to the 4.2-MeV signal from the minimum ionization particle signals. The neutron-induced readout noise is about 7 keV, which is more than a factor of 4 smaller than that from the γ-rays.**

***Index Terms*— Gamma-ray, induced readout noise, $Lu_{2(1-x)}Y_{2x}SiO_5$ (LYSO), neutron, photocurrent, silicon photomultiplier (SiPM).**

I. Introduction

THE Compact Muon Solenoid (CMS) experiment has a comprehensive upgrade plan for the High-Luminosity Large Hadron Collider (HL-LHC) which will operate at a luminosity of 5×10^{34} cm^{-2}s^{-1} for 10 years with an integrated luminosity of 4000 fb^{-1} [1]. A minimum ionization particle (MIP)-based timing detector (MTD) is under construction to mitigate the severe pileup effect expected at the HL-LHC [2]. Bright and fast cerium-doped lutetium–yttrium oxyorthosilicate ($Lu_{2(1-x)}Y_{2x}SiO_5$:Ce, LYSO or LYSO:Ce) crystals readout by silicon photomultiplier (SiPM) are planned to be used in the barrel timing layer (BTL) of the MTD. Recent studies show that LYSO crystals are radiation hard against γ-rays [3], charged hadrons [4], [5], and neutrons [6]. However, it is also important to understand radiation-induced readout noise (RIN) in the LYSO+SiPM packages from the γ-rays and neutrons expected *in situ* at the HL-LHC. These types of RIN measurements were first used for CMS lead tungstate (PWO or $PbWO_4$) crystal quality control [7]–[9] and subsequently in Caesium Iodide (CsI) quality assurance by the Mu2e experiment at Fermi National Accelerator Laboratory (Fermilab), Batavia, IL, USA [10]–[12].

Manuscript received March 11, 2021; revised April 15, 2021; accepted April 18, 2021. Date of publication April 27, 2021; date of current version June 14, 2021. This work was supported in part by the U.S. Department of Energy, Office of Science, Office of High Energy Physics, under Award DE-SC0011925, in part by Fermilab under Grant PO#661273, and in part by Prime DOE under Grant DE-AC02-07CH11359.

The authors are with HEP, California Institute of Technology, Pasadena, CA 91125 USA (e-mail: zhu@hep.caltech.edu).

Color versions of one or more figures in this article are available at https://doi.org/10.1109/TNS.2021.3075943.

Digital Object Identifier 10.1109/TNS.2021.3075943

Table I lists the integrated hadron fluence and γ-ray dose as a function of pseudorapidity (η), which are expected by the CMS MTD detector after 10 years. Also listed in Table I are the expected hadron flux and γ-ray dose rate. The numerical values in Table I were calculated by using the CMS beam radiation instrumentation and luminosity (BRIL) tool [13] where the neutron fluence is shown in 1-MeV neutron equivalent in silicon. We notice that the BTL LYSO+SiPM packages expect up to a dose rate of about 200 rad/h and a 1-MeV neutron equivalent flux of 3.2×10^6 cm^{-2}s^{-1} at the highest pseudorapidity of $\eta = 1.45$ (bold in Table I).

In this article, we report the results of an investigation on RIN induced by γ-rays (RIN:γ) and neutrons (RIN:n) in LYSO+SiPM packages. SiPM current before, during, and after irradiation by γ-rays and neutrons was measured by an SiPM coupled to LYSO crystal bars from several vendors for a dose rate of up to 250 rad/h and a neutron flux of 8.2×10^5 n_{eq}/cm^2/s. The photocurrent measured during irradiation was used to extract the energy equivalent readout noise RIN for LYSO+SiPM packages. The correlation between the RIN value and the crystal light output (LO) was also reported.

II. Experimental Details

Fig. 1 shows particle energy spectra for neutron (left), photons, and charged hadrons (right) expected at the LHC, which are calculated by using the CMS BRIL tool. Both γ-rays and neutrons are peaked at several MeV, which is in a good agreement with the energies of γ-rays and neutrons from Co-60 and Cf-252 radioactive sources, respectively. We thus used Co-60 and Cf-252 as the radiation source for the RIN:γ and RIN:n investigations, respectively.

Fig. 2 shows a setup used to measure photocurrent induced in LYSO+SiPM packages under irradiation from a Co-60 γ-ray source or a Cf-252 neutron source. Four LYSO crystal bars of $3.12 \times 3.12 \times 57.00$ mm^3 randomly picked from a batch of 20 samples from each vendor produced by Crystal Photonics, Inc. (CPI) (CPI-12), Shanghai Institute of Ceramics (SIC) (SIC-5), and Sichuan Tianle Photonics Co., Ltd. (Tianle) (Tianle-2 and Tianle-20) were used in this investigation [14]. The sample Tianle-20 shows a decay time of about 34 ns that is shorter than 40 ns from the other three samples. Both γ-ray and neutron irradiation were carried following the order of CPI-12, SIC-5, Tianle-2, and Tianle-20. The samples under irradiation were surrounded by a Teflon block and coupled with an air gap to a Hamamatsu S14160-3015PS SiPM at -40 V (2-V overvoltage) with a gain of 2×10^5. The SiPM current was measured by a Keithley 6485 picoammeter.

TABLE I
RADIATION ENVIRONMENT EXPECTED BY THE CMS MTD DETECTOR AFTER 4000 fb^{-1} AT THE HL-LHC

CMS MTD	η	n_{eq} (n_{eq}/cm^2)	n_{eq} Flux ($n_{eq}/cm^2/s$)	Protons (p/cm^2)	p Flux ($p/cm^2/s$)	Dose (Mrad)	Dose rate (rad/h)
Barrel	0.00	2.5×10^{14}	2.8×10^{6}	2.2×10^{13}	2.4×10^{5}	2.7	108
Barrel	1.15	2.7×10^{14}	3.0×10^{6}	2.4×10^{13}	2.6×10^{5}	3.8	150
Barrel	**1.45**	$\mathbf{2.9\times10^{14}}$	$\mathbf{3.2\times10^{6}}$	$\mathbf{2.5\times10^{13}}$	$\mathbf{2.8\times10^{5}}$	**4.8**	**192**
Endcap	1.60	2.3×10^{14}	2.5×10^{6}	2.0×10^{13}	2.2×10^{5}	2.9	114
Endcap	2.00	4.5×10^{14}	5.0×10^{6}	3.9×10^{13}	4.4×10^{5}	7.5	300
Endcap	2.50	1.1×10^{15}	1.3×10^{7}	9.9×10^{13}	1.1×10^{6}	26	1020
Endcap	3.00	2.4×10^{15}	2.7×10^{7}	2.1×10^{14}	2.3×10^{6}	68	2700

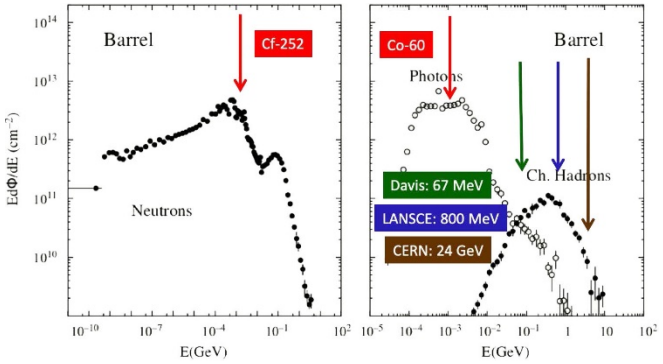

Fig. 1. Energy spectra for neutrons (left) and photons and charged hadrons (right) expected at LHC calculated by BRIL simulation [13] compared to Co-60 and Cf-252 radioactive sources and three proton accelerators.

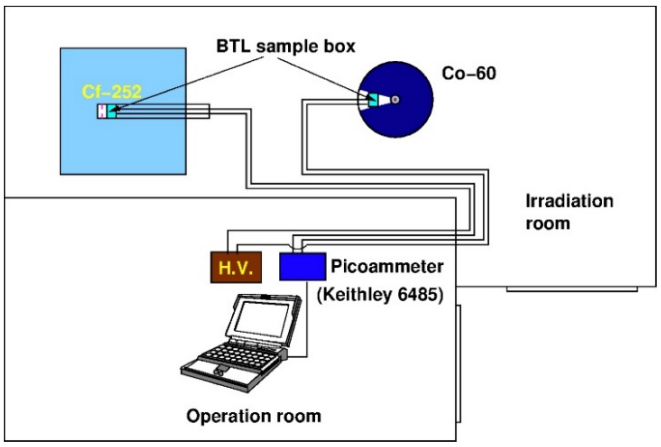

Fig. 2. Schematic showing the setup used to measure photocurrent in LYSO+SiPM packages induced by Co-60 γ-rays and Cf-252 neutrons.

The accuracy of the picoammeter is 0.2% + 10 pA for 20–200-nA range, 0.15% + 100 pA for 0.2–2-μA range, and 0.1% + 1 nA for 2–20-μA range.

The RIN:γ experiment was carried out first. LYSO+SiPM packages were placed at three positions from the Co-60 source of 50 Ci with γ-ray dose rates of 120, 185, and 250 rad/h that were measured by an ionization chamber with an uncertainty of about 10%. The SiPM current was measured for about 40 and 120–220 s before irradiation, 50 and 120 s during irradiation, and 40 and 120–190 s after irradiation for each LYSO+SiPM package in the RIN:γ and RIN:n experiment, respectively. The time interval between different dose rates for one sample is about 5–7 min.

Fig. 3 shows the layout of the neutron source assembly consisting of three cylindrical Cf-252 source pairs of 5, 5, and 1 mg. These sources were arranged to provide the best tradeoff between the neutron flux and the uniformity along the 57-mm-long LYSO bar.

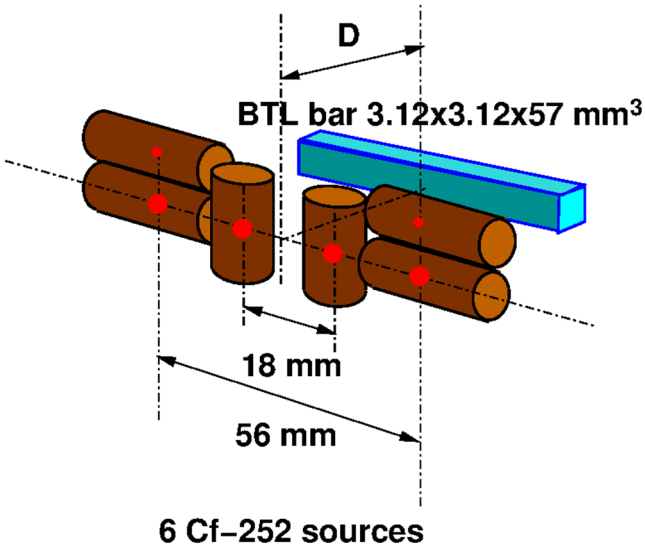

Fig. 3. Three Cf-252 source pairs are arranged to provide the best tradeoff between the intensity and the uniformity of the neutron flux applied to the 57-mm-long LYSO bar.

Fig. 4 shows the calculated neutron flux as a function of the position along the LYSO bar, which was placed at D = 1.4 cm from the source group with its center at $x = 5$ cm. The neutron flux of 8.2×10^5 $n_{eq}/cm^2/s$ applied to the entire LYSO bar from x = 2.15–7.85 cm was rather uniform with an rms of 4.2%. The γ-ray background was measured to be 2 rad/h by using the same ionization chamber used in the RIN:γ experiment.

The measured photocurrent was used to extract an F factor for the LYSO+SiPM package, defined as the radiation-induced photoelectron numbers per second, normalized to the γ-ray dose rate (F_γ) or neutron flux (F_n)

$$F = \frac{\frac{\text{Photocurrent}}{\text{Charge}_{\text{electron}} \times \text{Gain}_{\text{SiPM}}}}{\text{Dose rate}_{\gamma\,-\text{ray}} \text{ or } \text{Flux}_{\text{neutron}}}. \quad (1)$$

The photoelectron numbers (Q) in an integration gate were calculated by multiplying the F factor, the gate length, and the dose rate or neutron flux, which are 200 ns, 200 rad/h, or 3.2×10^6 $n_{eq}/cm^2/s$ for the CMS BTL detector

$$Q = F \times \text{Gate len.} \times \text{Dose rate}_{\gamma\,-\text{ray}} \text{ or } \text{Flux}_{\text{neutron}}. \quad (2)$$

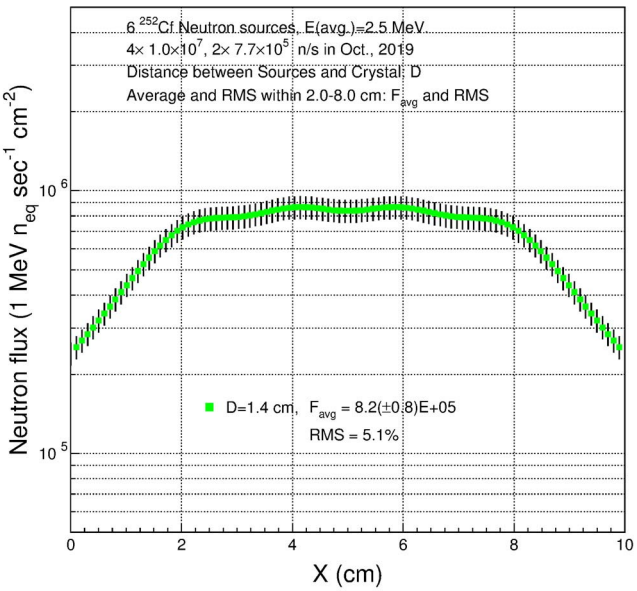

Fig. 4. Neutron flux is shown as a function of the position along the LYSO sample placed at $D = 14$ cm from the source group with its center at $x = 5$ cm.

The corresponding energy equivalent RIN:γ (σ_γ) or RIN:n (σ_n) values in keV under a dose rate or a neutron flux were calculated by normalizing the fluctuation of the photoelectron numbers Q to the measured LO in photoelectron numbers per MeV energy deposition for the corresponding LYSO+SiPM package. We note that the correlated noise due to crosstalk and after-pulse is negligible at 2-V overvoltage [15]:

$$\sigma\,(\text{keV}) = \frac{\sqrt{Q}}{\text{LO}\left(\frac{N_{\text{p.e.}}}{\text{MeV}}\right)} \times 1000. \tag{3}$$

III. Results and Discussion

A. Radiation-Induced Noise by Gamma-Rays

Fig. 5 shows histories of the photocurrent measured by the Hamamatsu S14160-3015PS SiPM under Co-60 irradiation with dose rates of 120, 185, and 250 rad/h. Also shown in Fig. 5 is the numerical values of the average SiPM photocurrent before, during, and 20 s after irradiation. The photocurrent during irradiation is 119, 163, and 217 nA for the dose rates of 120, 185, and 250 rad/h, respectively. We notice no significant variation between dark currents measured before and after three irradiation steps, indicating negligible damage in the SiPM by 35 rad from Co-60 γ-rays.

Figs. 6 and 7 show histories of photocurrent measured for four LYSO+SiPM packages under Co-60 irradiation of 120, 185, and 250 rad/h. Also listed in Figs. 6 and 7 are the numerical values of the average SiPM photocurrent during irradiation ranging from 221 to 565 μA, which are more than three orders of magnitude larger than that for SiPM alone shown in Fig. 5. This indicates that radiation-induced scintillation light in LYSO crystals dominates the photocurrent in LYSO+SiPM packages.

The total dose was 7.8 rad for all crystals, except CPI LYSO-12, which received an additional dose of 3.4 rad for test runs. The corresponding LO loss in LYSO crystals during this experiment was negligible [3].

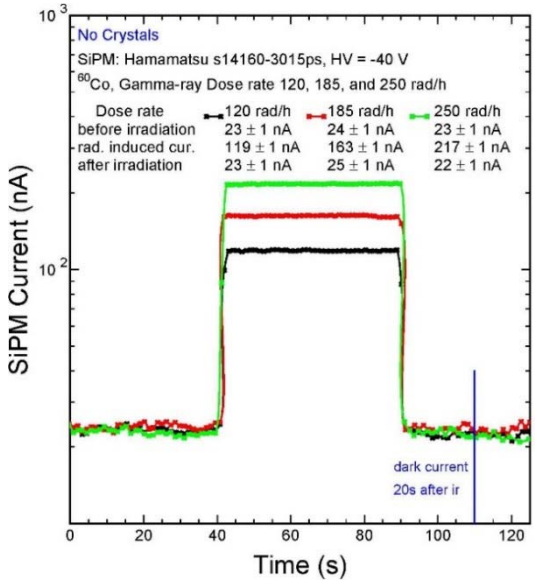

Fig. 5. Histories of the photocurrent measured for SiPM only under Co-60 irradiation of 120, 185, and 250 rad/h.

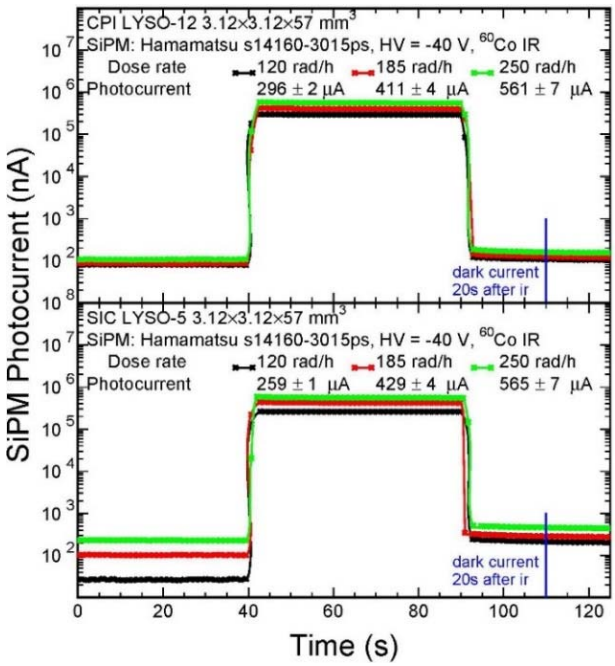

Fig. 6. Histories of photocurrent measured for CPI-12 (top) and SIC-5 (bottom) packages under Co-60 irradiation of 120, 185, and 250 rad/h.

Fig. 8 shows the photocurrent measured during irradiation as a function of the dose rate for four LYSO+SiPM packages, showing a good linearity with excellent correlation coefficients (CCs) of 99.7%, 99.0%, 99.4%, and 99.3%, respectively. Also listed in Fig. 8 are the numerical values of F_γ and RIN:γ (σ_γ). The F_γ factor values were calculated according to (1) by using the photocurrent during irradiation and the dose rate. The RIN:γ (σ_γ) values in a 200-ns gate were calculated according to (3) for the BTL detector under 200 rad/h. The LYSO crystal LO in a 200-ns gate was measured using a Hamamatsu R1306 Photomultiplier tube (PMT) and a LeCroy

TABLE II
SUMMARY OF PHOTOCURRENT, *F*-FACTOR, AND GAMMA-RAY-INDUCED READOUT NOISE FOR FOUR LYSO+SIPM PACKAGES

LYSO Crystal ID	L.O. of LYSO+SiPM (p.e./MeV)	Dose rate (rad/h)	Photocurrent before irrad. (nA)	Photocurrent during irrad. (μA)	Photocurrent 20s after irrad. (nA)	F_γ (p.e./s/(rad/h))	σ_γ (keV)
CPI-12	1610±16	120±12	81±1	296±2	108±1	$(7.2\pm0.2)\times10^7$	33.4±0.7
		185±19	87±1	411±4	108±1		
		250±25	107±1	561±7	159±2		
SIC-5	1620±16	120±12	27±1	259±1	125±1	$(7.0\pm0.2)\times10^7$	32.7±0.7
		185±19	103±1	429±4	288±3		
		250±25	230±2	565±7	460±5		
Tianle-2	1340±13	120±12	28±1	221±1	177±2	$(5.6\pm0.2)\times10^7$	35.6±0.8
		185±19	50±1	328±2	273±3		
		250±25	102±3	452±4	330±3		
Tianle-20	1480±15	120±12	27±1	246±1	101±1	$(6.4\pm0.2)\times10^7$	34.1±0.7
		185±19	45±1	388±3	153±2		
		250±25	71±2	497±5	191±2		

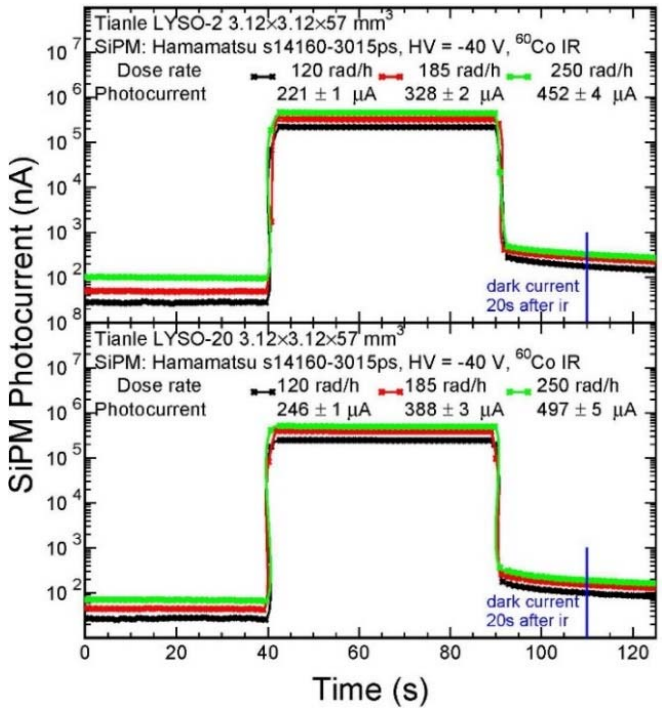

Fig. 7. Histories of photocurrent measured for Tianle-2 (top) and Tianle-20 (bottom) packages under Co-60 irradiation of 120, 185, and 250 rad/h.

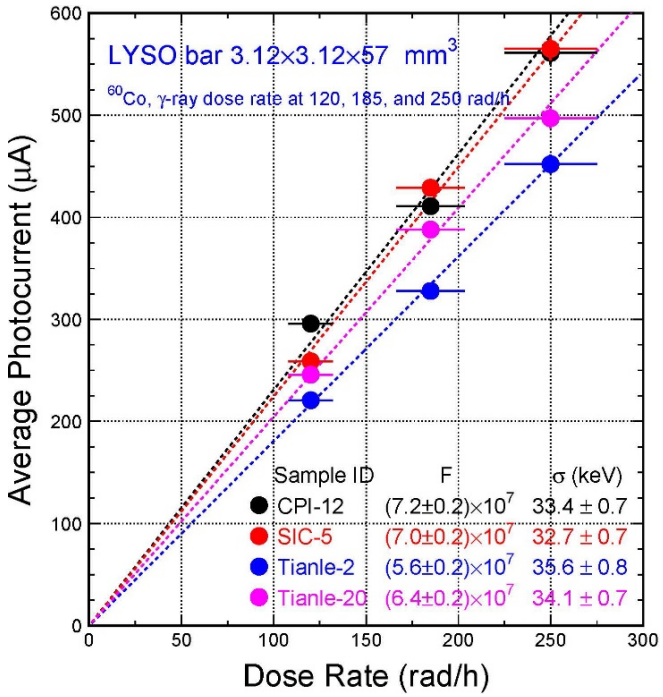

Fig. 8. Photocurrent as a function of dose rate for four LYSO+SiPM packages with numerical values of F_γ and RIN:γ under 200 rad/h listed.

3001 charge, voltage and timing multi-channal analyzer (QVT MCA) with coincidence triggers from a Na-22 source for each LYSO bar surrounded by the same Teflon block and coupled to the PMT with an air-gap [8]. The corresponding LO values for LYSO+SiPM packages were corrected for the differences between the quantum efficiency of the Hamamatsu R1306 PMT and the particle detection efficiency (PDE) of the Hamamatsu S14160-3015PS SiPM as well as the fraction of the areas of the LYSO bars covered by photodetectors.

Table II summarizes the LO in a 200-ns gate, the average photocurrent before (dark), during, and 20 s after (afterglow) irradiation of 120, 185, and 250 rad/h, F_γ and RIN:γ in keV for four LYSO+SiPM packages.

The dark current measured before irradiation is 27–230 nA which is larger than 23 nA for SiPM alone. This is due to the phosphorescence in LYSO from both natural radioactive isotope ^{176}Lu (a β-emitter) and the residual afterglow from previous irradiation. The dark current before the first irradiation under 120 rad/h is about 27 nA for all LYSO+SiPM packages, except 81 nA from CPI-12. This 81 nA is due to the afterglow from several test γ-ray irradiation runs before the first 120-rad/h irradiation for CPI-12. The contribution of the natural phosphorescence is about 4 nA after subtracting SiPM dark current, so is negligible.

The photocurrent measured 20 s after each irradiation (afterglow) ranged from 101 to 460 nA for four LYSO+SiPM packages, which is more than three orders of magnitude lower than the radiation-induced photocurrent, indicating that the afterglow effect to RIN:γ is small when compared to γ-ray dose-induced readout noise. The afterglow effect,

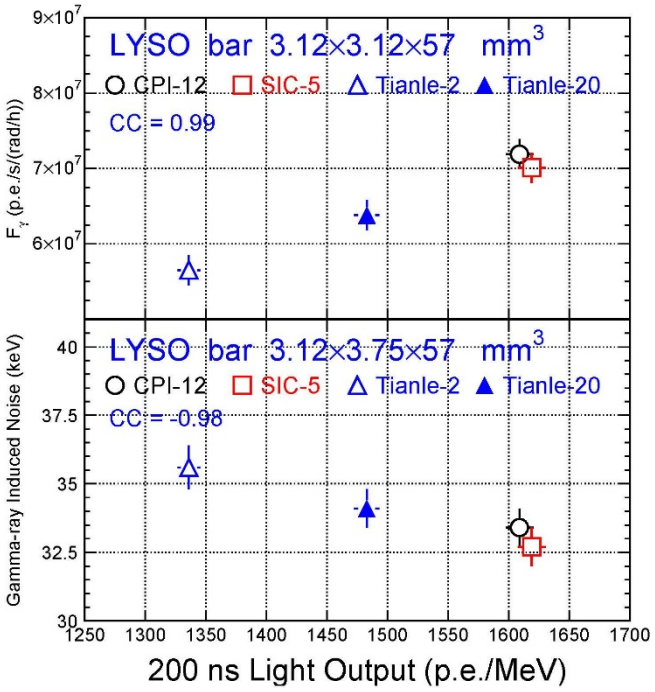

Fig. 9. Correlation between F_γ (top) and RIN:γ (bottom) versus LO in a 200-ns gate for four LYSO+SiPM packages.

however, is clearly shown in the larger dark currents measured before the second and third irradiations when compared to the first irradiation for each LYSO+SiPM package.

Fig. 9 shows an excellent correlation between the F_γ (top) and RIN:γ (bottom) versus the LO in a 200-ns gate for four LYSO+SiPM packages. The CC values of 99% and 98% confirm that the γ-ray-induced photocurrent and readout noise can be entirely attributed to the scintillation light from the LYSO crystals. The RIN:γ values are about 33 keV for all four LYSO+SiPM packages, which is less than 1% of the 4.2-MeV MIP signal in the CMS BTL detector.

B. Radiation-Induced Noise by Neutrons

Fig. 10 shows histories of the SiPM dark current measured during the entire neutron irradiation experiment with a flux of 8.2×10^5 $n_{eq}/cm^2/s$ from the Cf-252 source group, where the source ON (dashed lines) and OFF (solid lines) timing marks and the duration of each irradiation are shown. Also shown in Fig. 10 are the numerical values of the SiPM dark current before and after each step of irradiation and the corresponding neutron fluence.

While the SiPM current during the first 326 s of source ON is shown in Fig. 10, the photocurrent during the four irradiation periods of 121, 122, 124, and 122 s for four LYSO+SiPM packages are not shown in Fig. 10, rather in Figs. 12 and 13.

The SiPM dark current increased from 28 to 410 nA during the first step of 326 s after a neutron fluence of 2.7×10^8 n_{eq}/cm^2. It then stabilized at 390 nA due to thermal annealing at room temperature for about 20 min. We note that the dark currents measured are about one order of magnitude higher than in the RIN:γ experiment, indicating that the observed SiPM damage is dominated by neutrons.

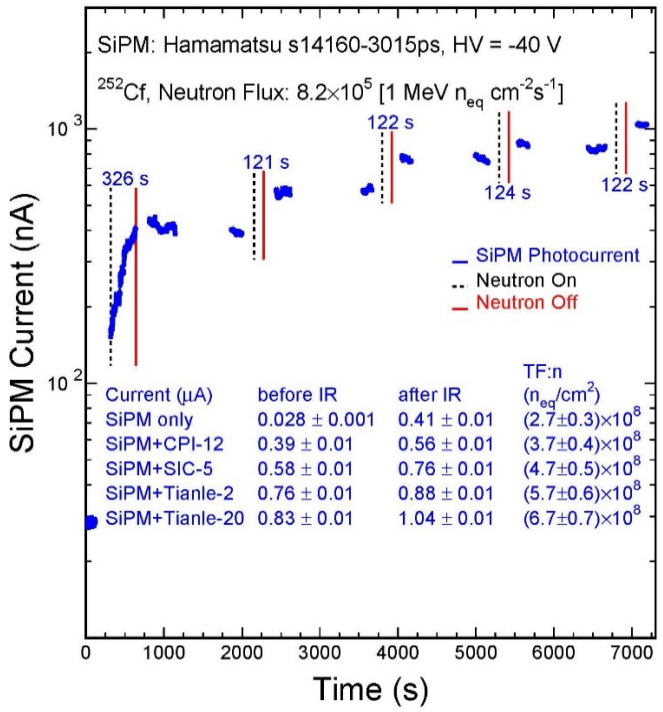

Fig. 10. Histories of SiPM current measured under the Cf-252 irradiation experiment.

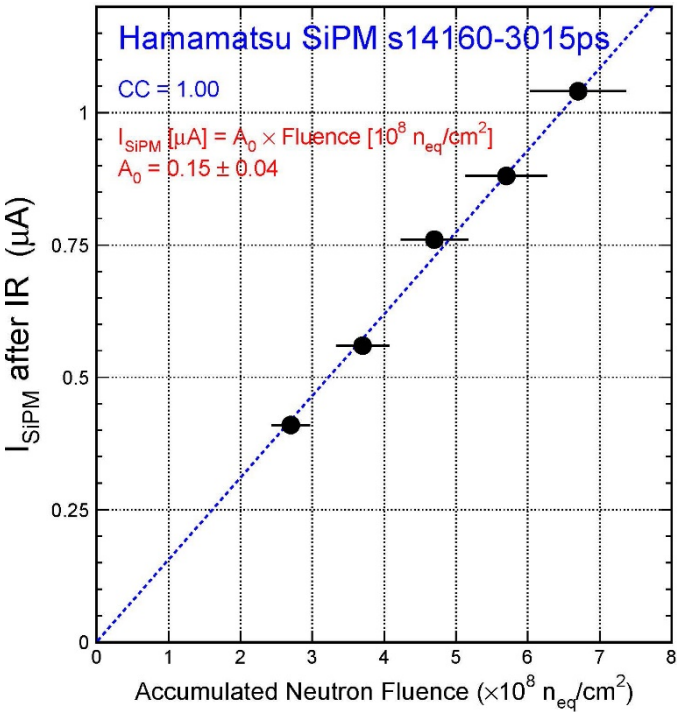

Fig. 11. SiPM dark current measured after each step of irradiation is shown as a function of the cumulated neutron fluence.

The SiPM dark current increased to 1.04 μA after a total fluence of 6.6×10^8 n_{eq}/cm^2 received in four irradiation steps for LYSO+SiPM packages. This steady increase of SiPM dark current shows clearly the evidence of cumulative damage in SiPM induced by neutrons [16]. Fig. 11 shows a good linearity between the SiPM dark current measured after five irradiation

TABLE III
SUMMARY OF CURRENT, F_n, AND NEUTRON-INDUCED READOUT NOISE FOR FOUR LYSO+SIPM PACKAGES

Crystal ID	L.O. of LYSO+SiPM (p.e./MeV)	Neutron Flux ($n_{eq}/cm^2/s$)	Photocurrent before irrad. (μA)	Photocurrent during irrad. (μA)	Photocurrent 20 s after irrad. (μA)	F_n (p.e./s/($cm^{-2}s^{-1}$))	σ_n (keV)
CPI-12	1610±16	(8.2±0.8)×10^5	0.39±0.01	10.0±0.1	0.56±0.01	188±6	6.8±0.1
SIC-5	1620±16	(8.2±0.8)×10^5	0.58±0.01	9.8±0.1	0.76±0.01	175±5	6.5±0.1
Tianle-2	1340±13	(8.2±0.8)×10^5	0.76±0.01	8.0±0.1	0.88±0.01	137±4	7.0±0.1
Tianle-20	1480±15	(8.2±0.8)×10^5	0.83±0.01	9.4±0.1	1.04±0.01	166±5	6.9±0.1

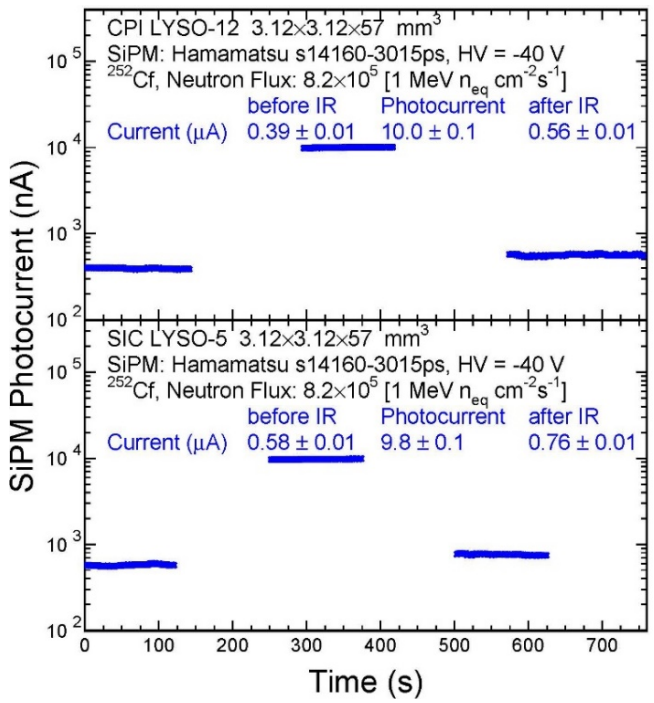

Fig. 12. Histories of photocurrent measured for CPI-12 (top) and SIC-5 (bottom) LYSO+SiPM packages under Cf-252 irradiation.

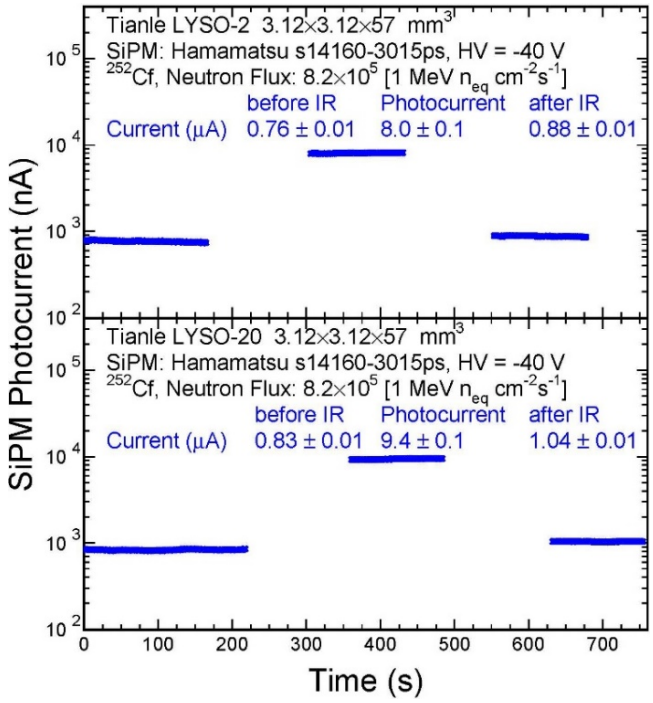

Fig. 13. Histories of photocurrent measured for Tianle-2 (top) and Tianle-20 (bottom) LYSO+SiPM packages under Cf-252 irradiation.

steps as a function of the cumulated neutron fluence. While such a linearity does not hold beyond 2 × 10^9 n_{eq}/cm^2, the high dark current expected by the BTL detector is a main concern. A mini thermal electric cooler (TEC) will be mounted on the SiPMs. The TEC allows SiPM operation at a low temperature, such as −35 °C or −45 °C, during beam ON to reduce the dark current, and at a high temperature, such as 25 °C, during beam OFF to facilitate thermal annealing [17].

Figs. 12 and 13 show histories of the photocurrent measured for four LYSO+SiPM packages under a neutron flux of 8.2 × 10^5 $n_{eq}/cm^2/s$ from the Cf-252 source group. Also listed in Figs. 12 and 13 are the numerical values of average photocurrent before, during, and after irradiation. The photocurrent measured during Cf-252 irradiation with a flux of 8.2 × 10^5 neq/cm^2/s is much lower than that measured during γ-ray irradiation, indicating that the main contribution to the RIN in LYSO+SiPM packages is from γ-rays *in situ* at the HL-LHC. The total neutron fluence received by LYSO bars in the RIN:n experiment is 9.8 × 10^7 n_{eq}/cm^2. The corresponding LO loss in LYSO crystals is also negligible [8].

Table III summarizes the LO in a 200-ns gate, average photocurrent before, during, and 20 s after Cf-252 irradiation under a neutron flux of 8.2 × 10^5 $n_{eq}/cm^2/s$, F_n and RIN:n in keV for four LYSO+SiPM packages. Table III also lists the F_n and RIN:n values calculated according to (1) and (3), respectively, for a neutron flux of 3.2 × 10^6 $n_{eq}/cm^2/s$ expected by the BTL at the HL-LHC. There are three contributions to the measured photocurrent during Cf-252 irradiation: dark current in SiPM, photocurrent induced by neutrons, and photocurrent induced by γ-ray background of 2 rad/h from the Cf-252 source, which was measured by using the same ionization chamber used in the RIN:γ experiment. Neutron-induced photocurrent was determined by subtracting the dark current in SiPM and the photocurrent induced by the γ-ray background, which was obtained by using (1) and the F factors extracted from the RIN:γ experiment for each LYSO+SiPM package.

Fig. 14 shows correlations between the F_n (top) and RIN:n (bottom) versus LO in a 200-ns gate for four LYSO+SiPM packages. The CC values of 95% and 82% confirm that the

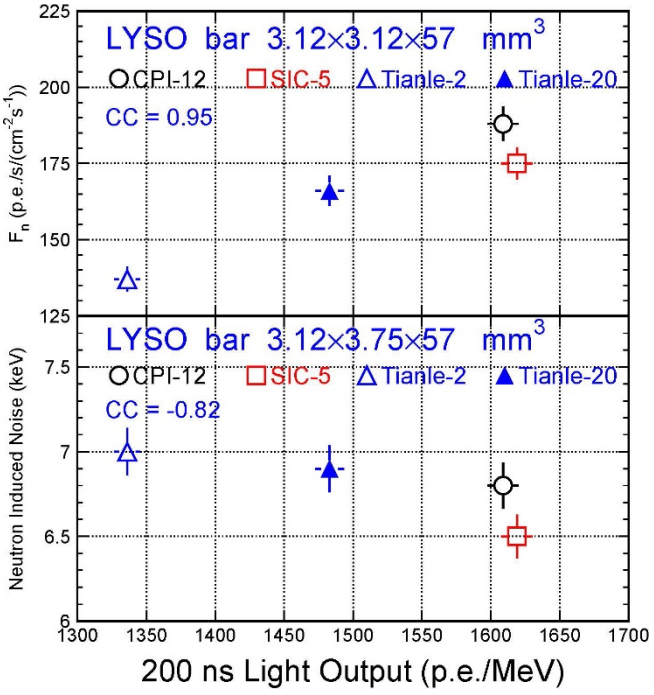

Fig. 14. Correlation between F_n (top) and RIN:n (bottom) versus LO in a 200-ns gate for four LYSO+SiPM packages.

neutron-induced photocurrent and readout noise are mostly due to the scintillation light from LYSO crystals as well. The result RIN:n value is found to be about 7 keV for four LYSO+SiPM packages under 3.2×10^6 $n_{eq}/cm^2/s$, which is more than a factor of 4 less than the 34 keV of RIN:γ under a γ-ray dose rate of 200 rad/h.

IV. Conclusion

RIN:γ and RIN:n experiments were carried out for four LYSO+SiPM packages under three γ-ray dose rates up to 250 rad/h and a neutron flux of 8.2×10^5 $n_{eq}/cm^2/s$. While these LYSO samples are not identical, they show consistent RIN:γ values of about approximately 33 keV for a 200-ns gate under the maximum γ-ray dose rate of 200 rad/h expected by the BTL detector at the HL-LHC, which is negligible when compared to the 4.2-MeV MIP signal. The RIN:n has a value of about 7 keV under the maximum neutron flux of 3.2×10^6 $n_{eq}/cm^2/s$, which is about a factor of 4 lower than the RIN:γ expected by the BTL detector at the HL-LHC, indicating that the dominant contribution to the RIN in LYSO+SiPM packages *in situ* at the HL-LHC is from γ-rays.

Good correlations are observed between the F and RIN values and the LO of the LYSO+SiPM package, indicating that radiation-induced photocurrent and readout noise are mainly due to scintillation light from LYSO crystals.

The use of LYSO+SiPM as a precision timing detector at the HL-LHC presents several technical challenges on the signal-to-noise ratio of the system. This investigation provides a solid evidence that radiation-induced noise would not be a show stopper. On the other hand, SiPMs are also known to suffer from increased dark current due to neutron-induced damage. This will be mitigated by mounting a TEC on the SiPMs for operation at low temperature during beam ON and annealing at high temperature during beam OFF.

Acknowledgment

The authors are grateful to the CMS collaborators, H. B. Newman, S. Xie, C. Peña, and the CMS Caltech Group for useful discussions and feedback. Maria Spiropulu thanks S. Miscetti and L. Bauerdick for early discussions on the project.

References

[1] *High-Luminosity LHC is a Major Upgrade of the Large Hadron Collider at CERN*, Geneva, Switzerland. [Online]. Available: https://home.cern/resources/faqs/high-luminosity-lhc

[2] J. Butler *et al.*, "A MIP timing detector for the CMS phase-2 upgrade," CMS Exp. CERN, Geneva, Switzerland, Tech. Rep. CERN-LHCC-2019-003, CMS-TDR-020, 2019.

[3] F. Yang, L. Zhang, and R.-Y. Zhu, "Gamma-ray induced radiation damage up to 340 Mrad in various scintillation crystals," *IEEE Trans. Nucl. Sci.*, vol. 63, no. 2, pp. 612–619, Apr. 2016.

[4] F. Yang, L. Zhang, R.-Y. Zhu, J. Kapustinsky, R. Nelson, and Z. Wang, "Proton-induced radiation damage in fast crystal scintillators," *IEEE Trans. Nucl. Sci.*, vol. 64, no. 1, pp. 665–672, Jan. 2017.

[5] C. Hu *et al.*, "Proton-induced radiation damage in BaF_2, LYSO, and PWO crystal scintillators," *IEEE Trans. Nucl. Sci.*, vol. 65, no. 4, pp. 1018–1024, Apr. 2018.

[6] C. Hu *et al.*, "Neutron-induced radiaion damage in LYSO, BaF_2, and PWO crystals," *IEEE Trans. Nucl. Sci.*, vol. 67, no. 6, pp. 1086–1092, Jun. 2020.

[7] R. Mao, L. Zhang, and R.-Y. Zhu, "Gamma ray induced radiation damage in PWO and LSO/LYSO crystals," in *Proc. IEEE Nucl. Sci. Symp. Conf. Rec. (NSS/MIC)*, Oct. 2009, pp. 2045–2049.

[8] L. Zhang, R. Mao, and R.-Y. Zhu, "Effects of neutron irradiations in various crystal samples of large size for future crystal calorimeter," in *Proc. IEEE Nucl. Sci. Symp. Conf. Rec. (NSS/MIC)*, Oct. 2009, pp. 2041–2044.

[9] R.-Y. Zhu, "Radiation damage effect," in *Handbook of Particle Detection and Imaging*, I. Fleck *et al.*, Eds. Cham, Switzerland: Springer, 2020. [Online]. Available: https://link.springer.com/referenceworkentry/10.1007/978-3-319-47999-6_22-2

[10] N. Atanov *et al.*, "Quality assurance on undoped CsI crystals for the Mu_2e experiment," *IEEE Trans. Nucl. Sci.*, vol. 65, no. 2, pp. 752–757, Feb. 2018.

[11] F. Yang, L. Zhang, C. Hu, and R.-Y. Zhu, "Slow scintillation component and radiation-induced readout noise in undoped CsI crystals," *IEEE Trans. Nucl. Sci.*, vol. 65, no. 10, pp. 2716–2723, Oct. 2018.

[12] C. Leroy, P.-G. Rancoita, *Principles of Radiation Interaction in Matter and Detection*, 4th ed. Singapore: World Scientific, 2016, pp. 477–567.

[13] "FLUKA particle flux maps for CMS detector," CMS Collaboration, CMS Exp. CERN, Geneva, Switzerland, CMS Performance Note CMS-DP-2013-028, 2013.

[14] C. Hu *et al.*, "Characterization of sixty LYSO bars from three vendors for radiation damage tests," presented at the CMS MTD Barrel Sensor Meeting CERN, Oct. 2019. [Online]. Available: http://www.hep.caltech.edu/~zhu/talks/4CMS_191015_60_LYSO.pdf

[15] O. Girard, G. Haefeli, A. Kuonen, L. Pescatore, O. Schneider, and M. E. Stramaglia, "Characterisation of silicon photomultipliers based on statistical analysis of pulse-shape and time distributions," 2018, *arXiv:1808.05775*. [Online]. Available: http://arxiv.org/abs/1808.05775

[16] E. Garuttia and Y. Musienko, "Radiation damage of SiPMs," in *Proc. NIMA*, 2019, pp. 69–84.

[17] A. Heering, A. Karneyeu, and Y. Musienko, "Integration of mini TECs on the CMS MTD barrel timing layer 16 CH SiPM array to reduce the DCR after very high irradiation," presented in the CPAD Instrum. Frontier Workshop, 2021. [Online]. Available: https://indico.fnal.gov/event/46746/timetable/#20210318

[18] B. Biró *et al.*, "A comparison of the effects of neutron and gamma radiation in silicon photomultipliers," 2018, *arXiv:1809.04594*. [Online]. Available: http://arxiv.org/abs/1809.04594